








Open Archive Toulouse Archive Ouverte

OATAO is an open access repository that collects the work of Toulouse researchers and makes it freely available over the web where possible

This is an author's version published in: <http://oatao.univ-toulouse.fr/25915>

To cite this version:

Bonnet, Maxime  and Lefèvre, Yvan  and Llibre, Jean-François  and Harribey, Dominique  and Defaÿ, François  and Sadowski, Nelson *3D magnetic field model of a permanent magnet ironless axial flux motor with additively manufactured non-active parts*. (2019) In: 19th edition of International Symposium on Electromagnetic Fields in Mechatronics, Electrical and Electronic Engineering (ISEF 2019), 29 August 2019 - 31 August 2019 (Nancy, France). (Unpublished) .

Any correspondence concerning this service should be sent to the repository administrator: tech-oatao@listes-diff.inp-toulouse.fr

3D Magnetic Field Model of a Permanent Magnet Ironless Axial Flux Motor with Additively Manufactured Non-Active Parts

M. Bonnet
Laplace Laboratory
Université de Toulouse
Toulouse, France

maxime.bonnet@laplace.univ-tlse.fr

Y. Lefevre
Laplace Laboratory
Université de Toulouse
Toulouse, France

yvan.lefevre@laplace.univ-tlse.fr

J.F. Llibre
Laplace Laboratory
Université de Toulouse
Toulouse, France

jean-francois.llibre@laplace.univ-tlse.fr

D. Harribey
Laplace Laboratory
Université de Toulouse
Toulouse, France

dominique.harribey@laplace.univ-tlse.fr

F. Defay
ISAE-SUPAERO
Université de Toulouse
Toulouse, France

francois.defay@isae-supaero.fr

N. Sadowski
Grucad Laboratory
Universidade Federal de Santa Catarina
Florianópolis, Brazil

nelson@grucad.ufsc.br

Abstract— A simulation model of an ironless Axial-Flux Permanent-Magnet (AFPM) machines is presented. Indeed as accurate analytical methods do not yet exist for ironless AFPM, 3D Finite Element Analysis (FEA) is required at each time of an operating point. The purpose of this article is to show that for any operating point of the motor, the torque can be calculated from the distribution of the axial magnetic flux density obtained from only one 3D FEA. The proposed simulation model is validated by using a prototype of an AFPM ironless whose non-active parts are additively manufactured. This first step through the 3D printing technology is simplified by the use of cylindrical magnets and plastic mechanical supports.

Keywords—Axial flux motor, Magnetic field, additive manufacturing, Permanent Magnet, ironless

I. INTRODUCTION

In recent years, a new type of electric motor has emerged: the Axial Flux Permanent-Magnet (AFPM) motor. The growing interest in it is due to a higher torque density than conventional electric machines [1]. The interest of these motors can be found in many fields such as automotive [2], aeronautics [3], power generation [4] and for Unmanned Aerial Vehicles (UAVs) [5]. In all these applications, the AFPM is most of the time used in direct drive, improving the efficiency of the electromechanical chain. In addition, AFPMs can have several stators and/or rotors to increase the torque-to-weight ratio. However, the AFPM has some drawbacks. For example, the manufacture of iron parts can be complicated. A new type of axial motor has been specially designed to overcome manufacturing difficulties: the YASA motor [6]. Some of AFPM geometries allow the iron to be removed from the stator, reducing the weight of the motor without affecting too much its performances. Some of these motors, such as double-sided AFPM with internal stator, can be ironless at the stator and the rotor.

UAVs can take advantage of the benefits of AFPM. First, the AFPM is more compact than a radial flux motor, so for the same performance the embedded mass will be lower. Secondly, the AFPM has a high efficiency which will increase the autonomy in flight of the drone. The ironless AFPM has no cogging torque, so the torque ripples will be reduced, making the drone quieter.

Despite the advantages of AFPM, one important point remains to be taken into account: its theoretical study. Indeed,

due to its geometry, a 3D study is necessary. Two methods are mainly used to determine the magnetic field of an AFPM: a Finite Element Analysis (FEA) or sizing equations valid under several assumptions. Most often a combination of the two methods is used [1]-[7]. However, analytical solutions are starting to appear on AFPMs with iron [8] [9].

Ironless AFPMs are more difficult to model. Their analytical models require many assumptions to be used. The FEA method requires fewer assumptions and are more accurate. The interest is to assess the motor performances more confidently. However, the FEA is very expensive in computation time. As the magnetic field varies in space and time, to have the torque at one operating point several 3D FEAs are required. A simulation model based on only one 3D FEA is proposed in this paper.

II. SIMULATION MODEL BASED ON 3D FEA

A. Principle of the simulation model

In FEA the torque exerted is calculated using the Maxwell tensor. In this case, the total field due to the current and the permanent magnet (PM) needs to be known. As there is no iron in the studied motor (Fig. 1), the Lorentz law can be applied to calculate the torque exerted on the stator. Due to the action reaction principle, this torque is the opposite of the torque exerted on the rotor. In this case, only the magnetic field due to PM needs to be known. The torque is defined by:

$$\begin{aligned} C_{stator} &= -C_{rotor} \\ &= \iiint_{windings} \left[\vec{R} \wedge (\vec{j}(\vec{R}, t) \wedge \vec{B}(\vec{R}, t)) \right] \cdot \vec{e}_z dV \end{aligned} \quad (1)$$

The vector \vec{R} is the vector position of a point that undergoes a current density \vec{j} produced by the current supply and a magnetic flux density \vec{B} due to PMs. \vec{j} and \vec{B} change with space and time, so the torque must be calculated according to the position of the rotor and the evolution of the conductors over time. The development of (1) in a cylindrical coordinates tied to the stator leads to:

$$C_{rotor} = - \iiint_{windings} \left[\begin{matrix} r \\ 0 \\ z \end{matrix} \wedge \left(\begin{matrix} j_r \\ j_\theta \\ 0 \end{matrix} \wedge \begin{matrix} B_r \\ B_\theta \\ B_z \end{matrix} \right) \right] \cdot \vec{e}_z dV \quad (2)$$

B. Mapping the axial magnetic flux density

To test the method presented in the previous section, an AFPM ironless is proposed with two rotor discs and one

internal stator disc. The stator disc consists of two stages of coils, with a total of 12 coils. The motor therefore has two air gaps. The two rotors are identical, each containing 8 cylindrical PMs. The PMs are magnetized in the axial direction. To maximize flux density, neodymium iron boron (NdFeB) magnets are chosen. They are distributed on the rotor disk as shown in Fig. 1.

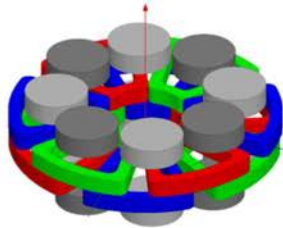


Fig. 1. Representation of the motor in ANSYS-Maxwell [10]

The chosen study domain is shown on Fig. 2 has a shape of a “piece of cake” containing one PM shown in red. The side walls, shown in blue, are linked by an anti-cyclic condition on the magnetic flux density: the azimuthal components of the magnetic flux density are opposite. The surface where the magnetic flux density is normal is shown in yellow (bottom surface). Eventually the surface bounding the study domain in the axial direction is placed far enough from the PMs. So the magnetic field strength can be assumed tangential (top surface). The axial component of the magnetic flux density B_z is then known. The torque can then be calculated with the formula (2)

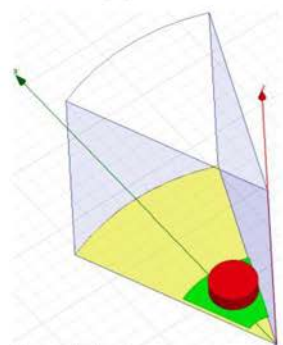


Fig. 2. The study domain consisting in one upper pole of the motor without the supports and windings

III. MEASURE AND EXPERIMENTAL VALIDATION

For one phase supply, the peak values of the static torque are presented in Table I. Fig. 3 shows the evolution of the static torque as a function of the rotor angle. C_{exp} is the static torque measured on the prototype. C_{3D} is the torque calculated by ANSYS-Maxwell 3D [10], thanks to the complete representation of the motor, as shown in Fig. 1. C_{th} is calculated by (2).

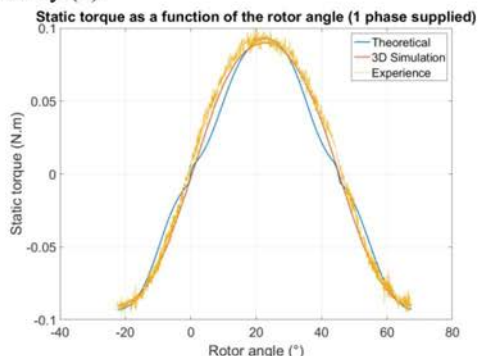


Fig. 3. Comparison of FEA methods for 1 phase supplied for $I = 10A$

TABLE I. RESULTS WITH ONE PHASE SUPPLIED

I (A)	3	5	7,5	10
C_{exp} (mN.m)	28,5	48,45	68,4	89,8
C_{3D} (mN.m)	27,25	45,36	68,01	90,66
C_{th} (mN.m)	27,8	46,4	69,6	92,8

IV. CONCLUSION

In this paper, it is shown that by a theoretical study of the torque, this torque could be calculated by a single mapping of the axial flux density done with 3D FEA. The results of this method have been validated by a classic FEA 3D study and by torque measurements performed on a prototype on a test bench. The static torque values obtained by the proposed method, the classic 3D FEA and measurements are very close, around 5% of relative difference for all the tests carried out. The proposed method allows good results to be obtained in a much shorter time. In addition, this method allows the torque, in function of the rotor position, to be calculated for any types of winding and any current waveshapes from only one axial flux density mapping.

The motor tests new manufacturing processes with additive manufacturing on non-active parts. This allows to be freer in the choice and shape of the active parts. Indeed, whatever the shape of these active parts, 3D printed supports will adapt to these active parts. This prototype was manufactured to test the 3D printing of plastic and to validate the calculation model of this paper, so it is not designed in an optimal way. A video demonstration is available online [11]. This video shows a version of the motor with iron yokes in the rotor discs.

REFERENCES

- [1] J. F. Gieras, R. Wang, and M. J. Kamper, “Axial Flux Permanent Magnet Brushless Machines,” 2nd ed. New York, NY, USA: Springer-Verlag, 2008.
- [2] N. Taran, V. Rallabandi, G. Heins, and D. M. Ionel, “Coreless and conventional axial flux permanent magnet motors for solar cars,” IEEE Trans. Ind. Appl., vol 54, no. 6, pp. 5907-5917, Nov./Dec. 2018.
- [3] Tallero T. F., Chin J. C. and Cameron Z. A., “Optimization of an Air Core Dual Halbach Array Axial Flux Rim Drive for Electric Aircraft,” in AIAA Aviation Forum, Atlanta, GA, USA, Jun. 23-29, 2018.
- [4] Subotic I., Gammeter C., Tüysüz A. and Kolar J. W., “Weight Optimization of Coreless Axial-Flux PM Machines,” IET Electric Power Applications, Oct. 16, 2018
- [5] G. Brando, A. Danner, A. Del Pizzo, and L.P. Di Noia, “A direct drive solution for contra-rotating propellers in electric unmanned aerial vehicle,” in Proc. Int. Conf. on Electrical Systems for Aircraft, Railway, Ship Propulsion and Road Vehicles, Aachen, Germany, 3-5 March 2015, pp. 1-6.
- [6] T. J. Woolmer and M. D. McCulloch, “Analysis of the yokeless and segmented armature machine,” in Proc. IEEE IEMDC, May 2007, pp. 704–708.
- [7] G. Weiwei and Z. Zhuoran, “Analysis and implementation of new ironless stator axial-flux permanent magnet machine with concentrated non-overlapping windings,” IEEE Transactions on Energy Conversion, vol. PP, no. 99, pp. 1–1, 2018.
- [8] T. Carpi, Y. Lefevre, C. Henaux, “Hybrid Modeling Method of Magnetic Field of Axial Flux Permanent Magnet Machine,” 2018 XXIII International Conference on Electrical Machines (ICEM), Alexandroupoli, Greece Sept. 2018.
- [9] J. F. Charpentier, F. Scullier, “3D Fast Calculation of Double Stator Axial Flux PM Machines with Ironless Rotor: experimental validation,” ,” 2018 XXIII International Conference on Electrical Machines (ICEM), Alexandroupoli, Greece Sept. 2018.
- [10] ANSYS Mechanical APDL Low Frequency Electromagnetic Analysis 215 Guide. Release 17.2, document, Aug. 2016.
- [11] Harribe D., “3D printed axial brushless motor for drones,” Youtube: <https://www.youtube.com/watch?v=JkwLpAABVVI>, Mar. 7, 2017